

W. WASILEWSKI✉  
P. WASYLCZYK  
C. RADZEWICZ

# Femtosecond laser pulses measured with a photodiode – FROG revisited

Institute of Experimental Physics, Warsaw University, Hoża 69, 00-681 Warsaw, Poland

Received: 4 November 2003 / Revised version: 9 December 2003  
Published online: 13 February 2004 • © Springer-Verlag 2004

**ABSTRACT** We demonstrate complete characterization of a femtosecond laser pulse electric field amplitude and phase using a FROG setup with a thick second harmonic crystal and a photodiode replacing a spectrometer. The scheme we propose is intended for high-repetition-rate pulse trains. It takes advantage of the photodiode high dynamic range and can be implemented in a compact size.

PACS 42.65.Ky; 42.65.Re

## 1 Introduction

Femtosecond lasers paved their way into many laboratories in the early 80's of the last century. Since then, characterizing pulses of femtosecond duration has become an important issue for numerous applications. Among early techniques used in this field, allowing for estimation of the pulse temporal duration, was the autocorrelation measurement. It was only at the beginning of the 90's that more advanced techniques, allowing for complete pulse characterization, were demonstrated. Two such methods, namely Frequency Resolved Optical Gating (FROG), invented by Trebino and coworkers [1], and Spectral Interferometry for Direct E-field Reconstruction (SPIDER), proposed and implemented by Walmsley and coworkers [2], are now the most popular. Commercial instruments based on these two methods are also available.

The FROG technique, in one of its numerous incarnations, is based on measuring spectra of pulses obtained by mixing two delayed pulse replicas in a second harmonic generation (SHG) crystal. The two-dimensional FROG spectrogram (SH intensity vs. delay and frequency) is a unique footprint of the ultrashort pulse under investigation [6], and application of a suitable algorithm allows one to retrieve the pulse temporal (or spectral) intensity and phase [7].

The physical idea behind the solution presented here is the long-ago realized fact that a thick SHG crystal acts as a spectral filter on the output wave [8, 9]. With femtosecond pulses, one needs moderate spectral resolution of the spectrograph used in a FROG setup, and thus the spectrograph can be

replaced with a reasonably thick (a few mm) nonlinear crystal. This scheme was first presented by us [3] and by Trebino et al. [4].

In this paper, we demonstrate how our original design can be further simplified for applications with high-repetition-rate sources such as femtosecond laser oscillators. We show that in this case the CCD array can be replaced with a single photodiode. This increases the dynamic range of the detection (by several orders of magnitude as compared to CCD cameras) and reduces the cost significantly. The device can be simplified even further because for the most common pulse lengths (20–200 fs) one can also eliminate expensive motorized translation stages.

## 2 SHG in a thick crystal

Let us consider the process of Type I second harmonic generation in an undepleted pump and plane wave approximation. Given two input fields  $E_1(\omega_1)$  and  $E_2(\omega_2)$ , the sum frequency field is [5]:

$$E_3(\omega) = \frac{\omega^2 \chi^{(2)}}{2c^2 k_e(\omega)} \int d\omega_1 d\omega_2 \delta(\omega_1 + \omega_2 - \omega) E_1(\omega_1) E_2(\omega_2) \times \frac{1 - \exp(i\Delta k(\omega_1, \omega_2)L)}{\Delta k(\omega_1, \omega_2)}, \quad (1)$$

where  $\chi^{(2)}$  is the second-order susceptibility,  $k_e$  is the wavevector of the resulting plane wave,  $\Delta k$  is the phase mismatch, and  $L$  is the medium thickness. To obtain an approximate formula for a thick nonlinear crystal, we expand  $\Delta k$  for the case of noncollinear interaction of two beams intersecting at an angle  $2\alpha$ :

$$\begin{aligned} \Delta k(\omega_1, \omega_2) &= k_o(\omega_1) \cos(\alpha) + k_o(\omega_2) \cos(\alpha) - k_e(\omega_1 + \omega_2) \\ &= (\beta_{1,o} \cos(\alpha) - \beta_{1,e})(\omega_1 + \omega_2 - 2\omega_0) \\ &\quad + \frac{1}{2} (\beta_{2,o} \cos(\alpha) + \beta_{2,e}) \\ &\quad \times ((\omega_1 - \omega_0)^2 + (\omega_2 - \omega_0)^2) \\ &\quad - \beta_{2,e}(\omega_1 - \omega_0)(\omega_2 - \omega_0) + \dots \end{aligned} \quad (2)$$

where  $\beta_{l,o} = \partial_\omega^l k_o(\omega)$ ,  $\beta_{l,e} = \partial_\omega^l k_e(\omega)$ , the subscripts o and e denote ordinary and extraordinary waves, respectively, and  $\omega_0$

is a frequency that is perfectly phase matched and depends on the crystal orientation ( $2\omega_0$  is the frequency of the corresponding second harmonic wave).

Neglecting the second- and higher-order terms in (2) leads to the expression for  $\Delta k$  as a function of  $\omega = \omega_1 + \omega_2$  only, thus in (1) the phase-mismatch factor can be taken outside the integral and the formula reads:

$$|E_{3,\text{thick}}(\omega)| \simeq \frac{\omega^2 \chi^{(2)}}{2c^2 k_e(\omega)} \times L \left| \text{sinc} \left( \frac{\pi(\omega - 2\omega_0)}{\delta\omega_f} \right) \right. \\ \left. \times \int d\omega_1 d\omega_2 \delta(\omega_1 + \omega_2 - \omega) E_1(\omega_1) E_2(\omega_2) \right|, \quad (3)$$

where

$$\delta\omega_f = \frac{2\pi}{L} \frac{1}{\beta_{1,e} \cos(\alpha) - \beta_{1,e}} \quad (4)$$

is approximately the full width at half maximum (FWHM) of the  $\text{sinc}^2$  function. Note that in the case of a thin crystal, when the phase mismatch is negligible, that is,  $L_{\text{thin}} \ll \pi/\Delta k_{\text{max}}$ , (3) simplifies to:

$$|E_{3,\text{thin}}(\omega)| \simeq \frac{\omega^2 \chi^{(2)}}{2c^2 k_e(\omega)} \times L_{\text{thin}} \\ \times \left| \int d\omega_1 d\omega_2 \delta(\omega_1 + \omega_2 - \omega) E_1(\omega_1) E_2(\omega_2) \right|. \quad (5)$$

This shows that  $E_{3,\text{thick}}$  is a spectrally-filtered version of  $E_{3,\text{thin}}$ . The filter central wavelength can be tuned by rotating the crystal, as this corresponds to selecting the wavelength that is perfectly phase matched ( $\omega_0$ ). For mixing two pulses centered at 800 nm, crossing in a KDP crystal of length  $L$  at an angle of  $3^\circ$ , the spectral filter width is  $\delta\lambda_f = 6.2 \text{ nm mm}/L$ .

Note that  $\beta_{1,e}$  and  $\beta_{1,o} \cos(\alpha)$  are the times it takes the second harmonic and fundamental pulses to travel a unit distance in the direction of the second harmonic propagation. Were these times the same, the bandwidth would be limited by higher-order expansion terms only [11].

The approximation used to obtain (3) is valid when the second-order expansion terms do not alter the phase-mismatch factor in (1) significantly, which is equivalent to requiring that  $L \sum_i \partial^2 \Delta k / \partial \omega_i^2 \Delta \omega_i^2 < \pi$ . If this is to be satisfied for input pulses with a spectral width  $\delta\omega_p$  (FWHM), the following must hold:

$$\delta\omega_p < 2 \sqrt{\frac{\pi}{L(\beta_{2,o} \cos(\alpha) + 2\beta_{2,e})}}. \quad (6)$$

$\theta$  (800 nm → 400 nm)       $45^\circ$

$\partial\theta/\partial\lambda$	0.037 %/nm
$\beta_{1,o}$	5.09 fs/ $\mu\text{m}$
$\beta_{2,o}$	0.0274 fs $^2$ / $\mu\text{m}$
$\beta_{1,e}$	5.16 fs/ $\mu\text{m}$
$\beta_{2,e}$	0.106 fs $^2$ / $\mu\text{m}$

TABLE 1 Material parameters for KDP crystal relevant in our method

For input pulses centered at 800 nm, mixed in KDP at an angle of a few degrees, this yields  $\delta\lambda_p < 80 \text{ nm} \sqrt{\text{mm}/L}$ . Again, notice that this inequality can be interpreted as a condition that neither of the pulses is distorted (lengthened) due to the material dispersion.

The above analysis has been carried out under an assumption that the interacting beams are plane waves. This is not the case in the experiment. The major effect associated with beam divergence is broadening of the spectral filter as the beam components propagating at finite angles to the beam axis see different crystal orientations.

The above results show that, indeed, one can substitute a thin crystal+spectrometer tandem with a thick crystal, provided that (6) is satisfied and  $\delta\omega_f$  is sufficiently small to resolve the spectrum of the second harmonic.

### 3 Experiment, results, and discussion

Our experimental setup is shown in Fig. 1. It contains a well-known rotating glass plate noncollinear autocorrelator [10]. Two parallel laser beams are formed in a Michelson interferometer and subsequently pass through a set of two 1 mm-thick glass plates mounted on an electric motor spindle. The plates are rotated by 90 degrees with respect to one another. The set of plates makes 11 revolutions per second, which corresponds to a 14 fs delay per 1  $\mu\text{s}$  in the rotation angle region where the delay is a linear function of the rotation angle and thus also a linear function of time. After passing the plates, the beams are focused and cross in a 3 mm-thick KDP crystal (experimentally we measure  $\delta\lambda_f \simeq 2 \text{ nm}$ , which is in good agreement with (4); that is, the broadening due to beam divergence is negligible). The latter is rotated by a stepper motor with a mechanical gear providing angular positioning in 10 arcmin steps. The resulting sum frequency beam is filtered spatially with an aperture and spectrally with a color glass filter to get rid of the fundamental beams as well as the parasitic second harmonic beams generated independently by each of the fundamental beams, and its intensity is measured with a photodiode.

In such an arrangement, the rotation of the plate assembly R (Fig. 1) changes the amount of glass the pulses travel

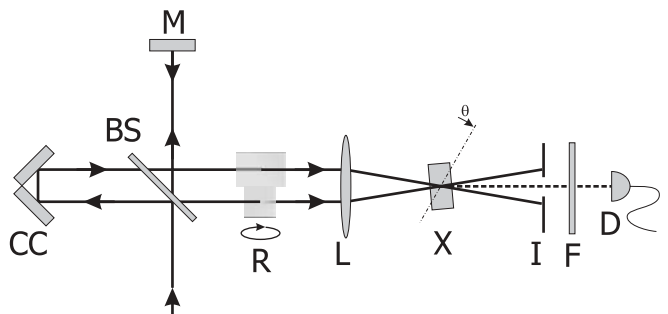


FIGURE 1 The experimental setup. The beam of pulses being measured is split into two with a beamsplitter BS. One pulse replica is reflected from the mirror M and passes through one of the glass plates of the rotating plates assembly R, while the other is reflected by the corner cube CC and passes through the other plate. The two pulse replicas are focused with a lens L ( $f = 200 \text{ mm}$ ) on a SHG crystal X (KDP, 3 mm), in which they intersect at an angle of  $3^\circ$ . An iris I and a color glass filter F cut out all the radiation but the summation beam, the intensity of which is measured with a photodiode D

through and thus the delay between the pulses in the upper and lower beams, while tilting of the optical axis of the crystal X changes the wavelength that the crystal filters out. Each acquisition of the spectrogram consists of recording up to 20 autocorrelation traces averaged for each SHG crystal angular position. The entire data acquisition takes up to two minutes for a single spectrogram.

As in other methods using crystal-angle dithering, there are two undesirable effects influencing the conversion efficiency. Besides selecting the phase-matched wavelength, the crystal rotation changes the effective path on which the beams interact, as well as the effective nonlinearity. The interaction length varies with  $1/\cos\theta$  of the tilting angle (inside the crystal) due to geometric effects, whereas the effective nonlinearity for the Type I process [13],  $d_{oe}$ , is proportional to  $\sin\theta$ , where  $\theta$  is the phasematching angle. In our case, since we rotate the crystal by no more than  $2^\circ$ , these are both small effects, the latter being dominant and not exceeding 2.5%.

To test our method, we used pulses generated by a home-built Ti : sapphire femtosecond oscillator operating at 800 nm. The pulses were stretched by passing the laser beam through a 51 mm-thick block of fused silica. We characterized them in a conventional (thin crystal+spectrometer) FROG setup and in our new setup. The pulses were retrieved from the recorded spectrograms with an error of 0.00075 for the conventional FROG and 0.0031 for our method.

We attribute the 4 times difference in error to the lower dynamics of the A/D converter (8 bit) we used with the photodiode compared to the 12 bit of the CCD camera in our conventional FROG. In addition, one should remember that the spectral filter imposed by the thick crystal is much broader than the spectrometer resolution. We estimate that the fastest instantaneous intensity variations our apparatus can resolve are on the time scale of the reciprocal of the filter bandwidth  $\delta t = 1/\delta\omega_f$ . From the agreement between the pulses retrieved from both measurements, we conclude that the spectral filtering in the properly chosen nonlinear crystal is narrow enough to record the correct FROG spectrogram.

The measured spectra and spectral phases are presented in Fig. 2. As one can see in the figure, the agreement between the two results is excellent – the phases do not differ by more than 0.05 rad even for spectral intensity as low as 5% of the maximum. Both retrieved spectra also agree well with the laser spectrum measured directly with a spectrometer.

The retrieved temporal intensity profiles are shown in Fig. 3. Both retrieved pulses have basically the same shape, including similar small kinks and other features. This indicates that our method is capable of retrieving complex pulse shapes.

It is interesting to compare the sensitivity of our method with that of a standard thin-crystal SHG FROG. Let us assume that the relative delay between pulses is fixed and the spectrum of the second harmonic is acquired in the range  $\Delta\omega$  with a resolution of  $\delta\omega$ , the same for both methods. If the pulses are mixed in a thin crystal and then a part of the spectrum centered around frequency  $\omega$  is registered with a detector (that is, a single CCD pixel), the number of photons collected by this detector during time  $T$  is proportional to:

$$S_{\text{thin}} = T |E_{3,\text{thin}}(\omega)|^2 \delta\omega. \quad (7)$$

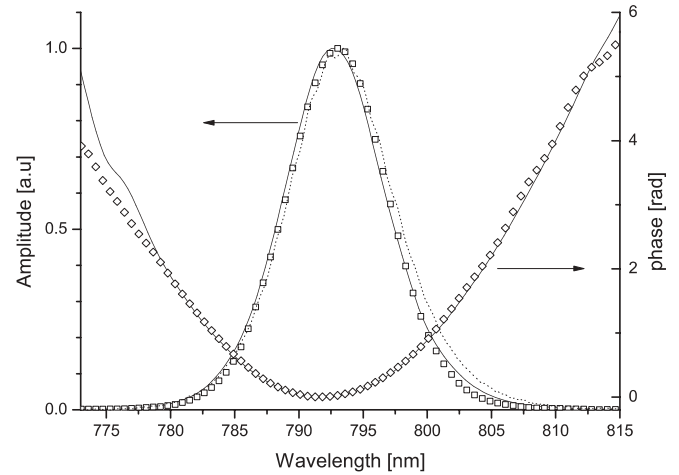


**FIGURE 2** Comparison of the pulse spectra and spectral phases retrieved from spectrograms measured in a standard thin-crystal FROG apparatus (lines), in our setup (squares and diamonds), and an independently measured pulse spectrum (dotted line). The spectral phase differences are below 0.05 rad for spectral intensity above 5% of the maximum

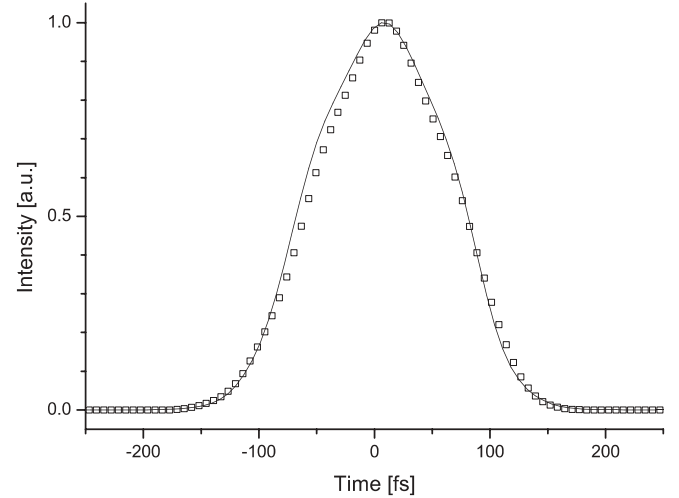


**FIGURE 3** Comparison of the pulses retrieved with a conventional FROG (line) and our setup (squares), in the time domain

The whole spectrum is registered simultaneously during the time  $T$ . In the thick-crystal case, one divides the measurement time  $T$  into  $N$  intervals, and during a single interval the intensity of the SH signal is measured with a photodiode. Then the crystal is rotated and another point of the SH spectrum is recorded. We assume that the crystal is rotated rapidly between measurements, so we can neglect the time required for that. During each time interval, the second harmonic intensity for frequencies centered around  $\omega$  is measured, and the number of photons collected is proportional to:

$$S_{\text{thick}} = \frac{T}{N} |E_{3,\text{thick}}(\omega)|^2 \delta\omega_f. \quad (8)$$

Using (3) and (5) and recalling that  $\delta\omega = \delta\omega_f$ , we obtain:

$$\frac{S_{\text{thick}}}{S_{\text{thin}}} = \left( \frac{L_{\text{thick}}}{L_{\text{thin}}} \right)^2 \frac{1}{N}. \quad (9)$$

In order to calculate the value of  $S_{\text{thick}}/S_{\text{thin}}$ , we have to estimate the maximum thickness of a thin crystal that can be used. This can be done by requiring that for such a crystal its SH bandwidth is sufficiently large; that is, the equality  $\delta\omega_f = \Delta\omega$  holds, which leads to:

$$N = \frac{\Delta\omega}{\delta\omega} = \frac{L_{\text{thick}}}{L_{\text{thin}}}, \quad (10)$$

and finally to:

$$\frac{S_{\text{thick}}}{S_{\text{thin}}} = N. \quad (11)$$

This shows that the FROG signal in our method can be many times bigger than the signal obtained with a conventional setup using a thin SH crystal and spectrometer. In our setup  $N \approx 20$ . This is a somewhat surprising result given that in our method the spectrum is acquired sequentially, as opposed to the simultaneous acquisition applied in the conventional method. However, the loss in the integration time is more than offset by signal increase due to increased SH conversion efficiency in a thick crystal. One should keep in mind that there is a limit on the crystal thickness, and thus the signal strength, imposed by (6).

Our device can be made as small as a fist. A matchbox-sized autocorrelator with minimized dispersion has been demonstrated recently [12], and one would only need to add a thick nonlinear crystal to that device to turn it into a compact setup for complete pulse diagnostics. With two galvos – one for controlling the double plate delay assembly and the other for rotating the crystal – it should be possible to build our setup in a very compact size. If the scan frequencies of both galvos are chosen properly, say 10 Hz and 500 Hz, respectively (resonant galvo scanners with frequencies up to 2000 Hz are commercially available), the device could provide a 10 Hz, live readout rate of the FROG spectrogram. To the best of our knowledge, this is the first solution offering this feature for low-intensity pulse trains and not relying on the spatial beam profile homogeneity.

## 4 Conclusion

We have demonstrated a new method to register the FROG spectrogram of a high-repetition-rate pulse train. The method relies on a thick nonlinear crystal for spectral filtering and a photodiode as the light detector. Femtosecond light pulses from a Ti : sapphire laser were characterized with the new method and a standard FROG was used as a reference. The retrieved pulse electric fields agree very well, from which we conclude that the thick nonlinear crystal indeed can be used as a spectral filter in the FROG method. A photodiode offers much higher dynamics than the CCD cameras found in many devices. Last but not least, it is the least expensive of all light detectors available. Moreover, the method offers a possibility to increase the acquisition rate up to a few hertz and to be implemented in a compact size.

**ACKNOWLEDGEMENTS** This research was supported in part by KBN Grant No. PBZ/KBN/043/P03/2001.

## REFERENCES

- 1 D.J. Kane, R. Trebino: IEEE J. Quantum Electron. **QE-29**, 571 (1993)
- 2 C. Iaconis, I.A. Walmsley: IEEE J. Quantum Electron. **QE-35**, 501 (1999)
- 3 C. Radzewicz, P. Wasylczyk, J. S. Krasinski: Opt. Commun. **186**, 329 (2000)
- 4 P. O'Shea, M. Kimmel, X. Gu, R. Trebino: Opt. Lett. **26**, 932 (2001)
- 5 M. Shubert, M. Wilhelmi: In *Nonlinear Optics and Quantum Electronics* (Wiley & Sons, New York 1986)
- 6 K.W. DeLong, R. Trebino, D.J. Kane: J. Opt. Soc. Am. B **11**, 1595 (1994)
- 7 K.W. DeLong, R. Trebino, J. Hunter, W.E. White: J. Opt. Soc. Am. B **11**, 2206 (1994)
- 8 A.G. Akmanov, A.I. Kovrigin, N.K. Podolskaya: Radio Engineering and Electron Physics **14**, 1315 (1969)
- 9 D.H. Auston: Opt. Commun. **3**, 272 (1971)
- 10 P. Wasylczyk: Opt. Appl. **30**, 121 (2000)
- 11 C. Radzewicz, Y.B. Band, G.W. Pearson, J.S. Krasinski: Opt. Commun. **117**, 295 (1995)
- 12 P. Wasylczyk: Rev. Sci. Instrum. **72**, 2221 (2001)
- 13 B.F. Levine, C.G. Bethea: Appl. Phys. Lett. **20**, 272 (1972)